Journal of Volcanology and Geothermal Research 346 (2017) 212–222

Contents lists available at ScienceDirect

Journal of Volcanology and Geothermal Research

journal homepage: www.elsevier.com/locate/jvolgeores

Possible mechanism of molten sulfur eruption: Implications from near-surface structures around of a crater on a flank of Mt. Shiretokoiozan, Hokkaido, Japan

Mutsunori Yamamoto [a,*], Tada-nori Goto [b], Michio Kiji [c]

[a] Earthscience.jp 2-11-7, Sakuradai, Minamitsutsujigaoka, Kameoka-shi, Kyoto 621-0847, Japan
[b] Graduate School of Engineering, Kyoto University C1-2-216, Kyotodaigaku-Katsura, Nishikyo-ku, Kyoto 615-8540, Japan
[c] Ritsumeikan Senior High School, 1-1-1 Choshi, Nagaokakyo 617-8577, Japan

ARTICLE INFO

Article history:
Received 25 May 2017
Received in revised form 9 November 2017
Accepted 10 November 2017
Available online 21 November 2017

Keywords:
Mt. Shiretokoiozan
Molten sulfur
Self-potential survey
Positive SP anomaly
DC resistivity survey

ABSTRACT

Shiretokoiozan volcano in northern Japan is well known for its eruptions, which eject huge amounts of molten sulfur. Watanabe (1940) reported details of the 1936 eruption, but its mechanisms, and how and where the huge amount of sulfur is produced and pushed out remain unknown. The aim of this study is to elucidate the near-surface underground structure of this area and the mechanisms of the molten sulfur eruption. We implemented aerial photographic observations, geological surveys, hot spring analysis, Self-Potential survey and DC resistivity surveys at the western flank of Mt. Shiretokoiozan. The geology of this area is mostly composed of hydrothermally altered boulders, gravels, sand, and clay. Some areas of fumaroles are covered by sulfur cement. Chemical analyses revealed that SO_4^{2-} and Cl^- are rich in hot water, which imply an area with upwelling hot water/gas below the surface. Results of DC resistivity surveys conducted at several sites show extremely low resistivity, suggesting an aquifer several meters below the surface. Compiling this evidence, we infer a possible mechanism of molten sulfur eruption: the sulfur has been produced and stored in an aquifer located at the eastern hill from Crater I for several decades by chemical reactions of volcanic gases; it gushes out when volcanic activity becomes high.

© 2017 The Authors. Published by Elsevier B.V. This is an open access article under the CC BY license (http://creativecommons.org/licenses/by/4.0/).

1. Introduction

Mt. Shiretokoiozan, a Quaternary andesitic composite volcano, located in the middle of the Shiretoko Peninsula, Hokkaido, is well known for its molten sulfur eruption. On the north-western flank of the volcano, the explosive activities were often recorded in the historical time around parasitic craters. In the beginning of the year 1936, one of the parasitic craters awakened from its quiet state, and began to erupt intermittently an abundant amount of molten sulfur, hot salty acid water and steam (Watanabe, 1940). A very interesting feature was the eruption of molten (hot liquid-state) sulfur, which continued about eight months after the first observation of the eruption. Watanabe and Shimotomai (1937) reported that 200,000 tons of molten sulfur were expelled at Crater I (Kadokura, 1919) on the northwestern side of the mountain, after which it flowed into Kamuiwakka Creek in 1936 and finally filled the valley about 1400 m of length. The Geological Survey of Japan (1967) reported the amount of sulfur mined and shipped between 1936 and 1943 as 116,523 tons (58,262 m^3). In addition, Watanabe (1940) reported a cyclic activity of the eruptions was recognized. At intervals of three to five days, thousand tons of molten sulfur were erupted from Crater I. The sulfur eruptions usually lasted 30 to 60 min, and about forty major eruptions were recorded during the entire period of the activity. In the intervening stage between major sulfur eruptions, the same crater (Crater I) played an ordinary geyser-like action and ejected intermittently hot acid water and steam (Watanabe, 1940). Yamamoto (2017) found rock-coating sulfur and tear-drop sulfur grains with air bubble cavities around Crater I. He also found that the sulfur pieces collected along the path of 1936-molten sulfur flow also have air bubble cavities. Those sulfur samples are evidences of explosive eruptions around Crater I, and imply that water vapor was contained in the molten sulfur and expanded the volume during the eruption.

Because of the highly pressurized condition of sulfur and the approximately four days' periodical (geyser-like) eruption, Watanabe (1940) speculated that there had been a chamber immediately beneath Crater I where all of molten sulfur was reserved and from which it had gushed out by water vapor pressure. If the chamber has a cylindrical shape and the diameter is similar to that of Crater I (40 m approximately), we can estimate the approximate chamber height as 46.4 m at least. If the chamber diameter becomes 80 m, the chamber height is at least 11.6 m. However, there are no evidences of such a huge chamber just

* Corresponding author.
E-mail addresses: yamamoto@earthscience.jp (M. Yamamoto), goto.tadanori.8a@kyoto-u.ac.jp (T. Goto), kjmcho@uranus.dti.ne.jp (M. Kiji).

https://doi.org/10.1016/j.jvolgeores.2017.11.009
0377-0273/© 2017 The Authors. Published by Elsevier B.V. This is an open access article under the CC BY license (http://creativecommons.org/licenses/by/4.0/).

beneath Crater I, holding reserves of molten sulfur with volume as large as 58,262 m^3 (=116,523 tons). Nobody also confirmed the upwelling flow of hot groundwater/gas beneath Crater I for providing large amount of sulfur to the huge chamber. Alternatively, there are expected to be other chambers or storage areas in other places where sulfur is generated and reserved, but their existence remains unknown.

The investigation of the molten sulfur eruption at Mt. Shiretokoiozan is important because it made one of the largest molten sulfur flows in the world. In terrestrial volcanism, small-scale sulfur flows are almost universal, and large-scale ones are observed although the frequency is very rare. Large sulfur eruptions are also found in volcanism occurring on Jupiter's satellite Io (e.g., Theilig, 1982). Unfortunately, sulfur lava flows have been described worldwide only in rare instances in a few reports (e.g., Watanabe, 1940; Skinner, 1970; Francis et al., 1980; Harris et al., 2000). As described by Francis et al. (1980) and Takano et al. (1994), it is believed that the presence of water in a crater lake plays an important role in sealing off the sulfur, preventing combustion or oxidation, and shaping the sulfur pool. However, no crater lakes were found on the northwestern side of Mt. Shiretokoiozan. Therefore, such mechanisms cannot explain the 1936 sulfur eruption.

This paper specifically examines how and where molten sulfur is generated and reserved. Since 2005, the authors have conducted studies at Mt. Shiretokoiozan. After studying the near-surface underground structure around Crater I, we propose a possible mechanism of molten sulfur eruption. The methods used for this study were multidisciplinary observations from aerial photographs, geological surveys, hot spring water analyses, self-potential surveys, and DC resistivity surveys. This study, which is also based on information referred from a report by Yamamoto and Goto (2015), includes information from further investigations.

2. Methods

Our target area is located on the northwestern side of the Mt. Shiretokoiozan including Crater I, Kamuiwakka Creek, and its vicinity (Fig. 1). Most of the mountain is covered by trees and grass, but the area near Crater I is characterized by its bare ground.

Four surveys were conducted as described below:

1. Observing aerial photographs and geological surveys
2. Geochemical analysis of hot springs
3. Self-Potential or Streaming Potential (SP) survey
4. DC resistivity survey

Results obtained from these multidisciplinary surveys were combined to elucidate groundwater conditions near the surface. Aerial photography with geological maps was used to identify detailed distributions of hot springs, fumaroles, and hydrothermal altered areas. DC resistivity surveys indicate the distributions of groundwater/gas near the surface. SP surveys can detect upwelling of groundwater and steam. Chemical analysis yields information related to solute transportation in groundwater.

2.1. Observing aerial photographs and geological surveys

Contact-printed aerial photographs CHO781-C2-20 (shown in Fig. 2) and CHO781-C2-21 were obtained from the Geospatial Information Authority of Japan. The photographs were taken from different points in the sky using a camera (RC10) with 23-cm wide film on October 9, 1978 at 2700 m above sea level.

Those aerial photographs were carefully scanned using a high-resolution scanner. Our target area was cut out of CHO781-C2-20; then exactly the same area was cut out of CHO781-C2-21. Those photographs were put side-by-side and enlarged to create a stereophotograph: a three-dimensional photograph.

Because our target area is composed mostly of hydrothermally altered white gravel and rock, the area in the photographs are too bright and too white to observe. Using image processing software, the aerial photograph brightness is adjusted so that colors on the ground are readily visible. In addition, a geological survey was administered in this study using a map made from the aerial photographs to create a precise geological map. As a result, a geological map (Fig. 3) is drawn both from observation of aerial photographs and actual geological surveys.

2.2. Hot springs analysis

In our field observations, hot springs were expelled mostly at the right bank (northern bank) of Kamuiwakka Creek. At Crater I, a hot spring formed temporarily in the summer 2013 and 2014 (Fig. 4). These events suggest clearly that hot spring water flows in an aquifer under Crater I and in its vicinity.

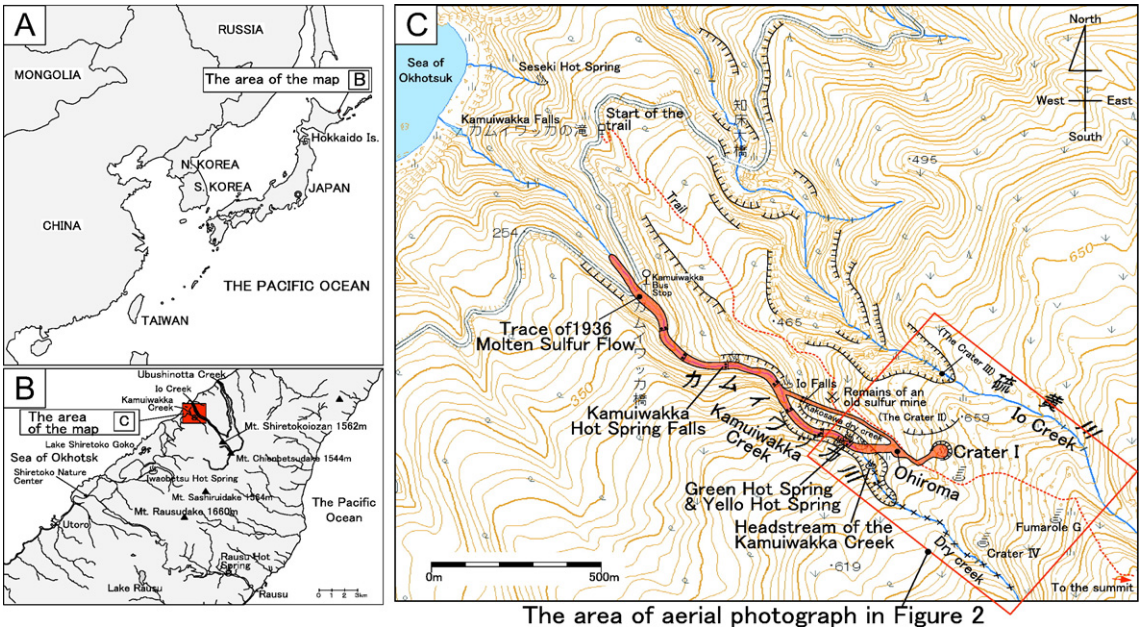

Fig. 1. Map of area around our research area.

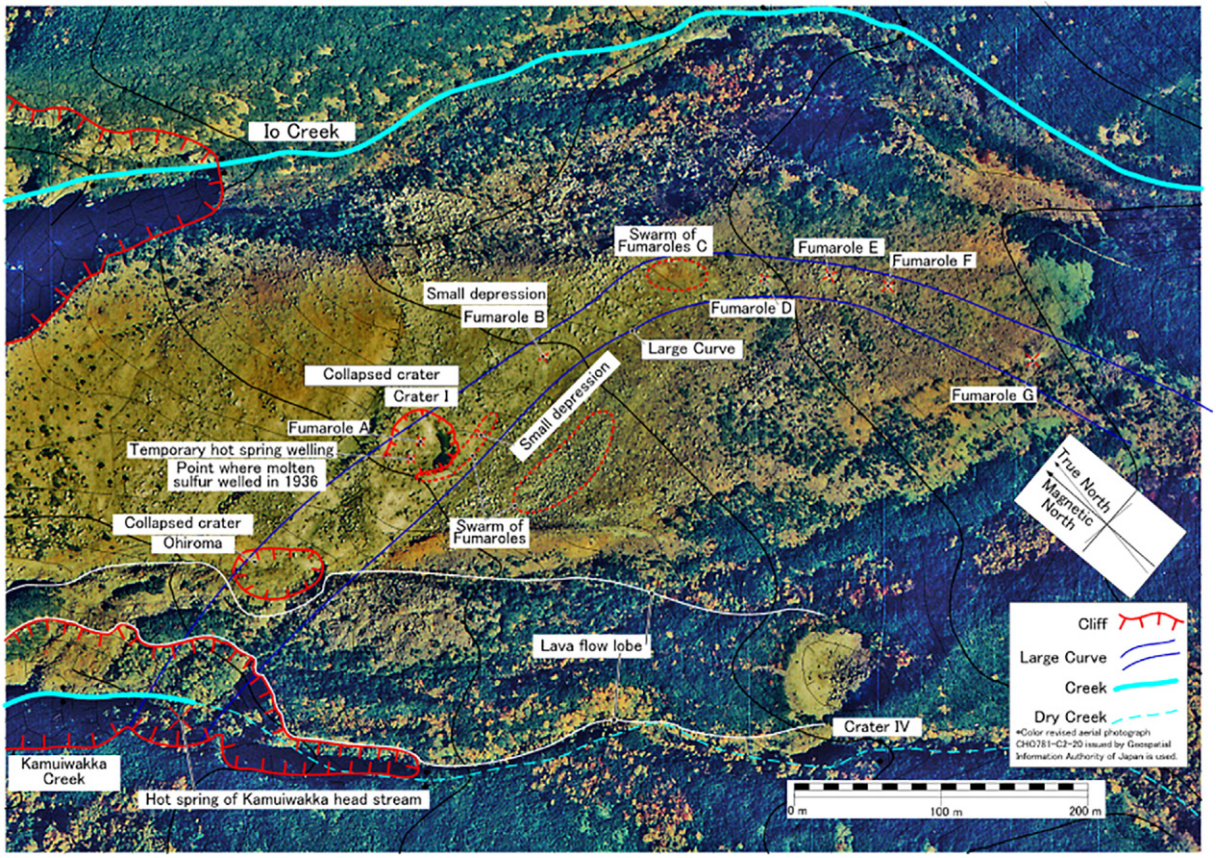

Fig. 2. Structural map developed from aerial photographs and field research. Aerial photographs CHO781-C2-20 from Geospatial Information Authority of Japan is used.

The hot spring water of Kamuiwakka Creek described in Table 1 was collected at the location marked in Fig. 4. The sample contains water from three hot springs. We designate the hot spring at the beginning of the stream as the "Head Stream." We designate the hot spring on the left cliff as the "Green Hot Spring," and on the right bank as the "Yellow Hot Spring."

Polyethylene bottles (250–500 cm^3) were used for collecting sample water. Before collecting the sample, the bottle was carefully washed using the hot spring water to be sampled. The bottle was tightly capped and carefully sealed after sampling the water. The sample temperatures were measured using a thermometer at the hot spring source. pH was measured temporarily using pH test paper and was later measured precisely at a laboratory. The temperature, pH, and the date of collection were recorded on the bottle before the bottle was put into a plastic bag. Samples were analyzed by the Kyoto Municipal Institute of Industrial Technology and Culture using ICP – atomic emission spectrometry and ion chromatography analysis.

2.3. Self-potential survey

Self-potential (SP) survey is a passive geophysical method based on measurement of the voltage differences in the ground. The quasi-static natural electrical potential, designated as SP, is thought to result from thermoelectric or electrochemical effects, or subsurface fluid flow through an electrokinetic coupling (e.g., Ishido, 1989). Emphasizing the correlation between SP and fluid flow, the spatial distribution of SP is useful for the mapping of geothermal heat sources and related hydrothermal activities (e.g., Corwin and Hoover, 1979; Zlotnicki and Nishida, 2003; Barde-Cabusson et al., 2012).

An SP survey was administered from the summer of 2013 through 2015 (three survey campaigns) to assess groundwater movements and heat anomalies. PET bottle electrodes (500 ml bottomless plastic bottle electrodes) were used for this study as described by Goto et al. (2012). The PET bottle electrode has a copper coil in a saturated copper sulfate solution which leaks slightly through the gypsum bottom and which electrically connects the circuit tester and ground. SP was measured using a digital multimeter. When the electrodes are sunlit, the SP value might be biased from the real value. Therefore, we prepared sun shading for each electrode. Our SP measurement was done by the conventional leap-frog method for cancelling the bias at electrodes. The measured potential differences between two electrodes are summed, and the raw SP distribution relative to a reference point can be obtained. The positions of electrodes were recorded carefully on the detailed map and by camera. Some of electrode locations are precisely shared among three survey campaigns for compiling SP data and for making one SP map relative to one common point (anchoring point).

Due to the corrosive environment, we placed two electrodes side by side for calibration, and checked the voltage offset between electrodes every day. If the value exceeds 5 mV, we exchanged an electrode to new one so that the value was kept below 5 mV. In addition, SP values along closed circles were measured at several areas for checking the drift of measured SP values. The drift value was about 0.1–0.4 mV/measurement (i.e., drift rate is about 0.005–0.04 mV/m since the measurement interval is about 10–20 m). The value was used for correction of drift in the raw SP values.

It was hard for us to achieve the SP survey in the whole area within one campaign. The SP measurement was implemented in August 2013 through July 2015, but fortunately, the discrepancies among the campaigns are not large. As shown in Fig. 5, you can find SP values closely plotted at almost same locations, which were obtained by different campaigns of SP survey. The differences of these values are small enough to be ignored in the later discussions.

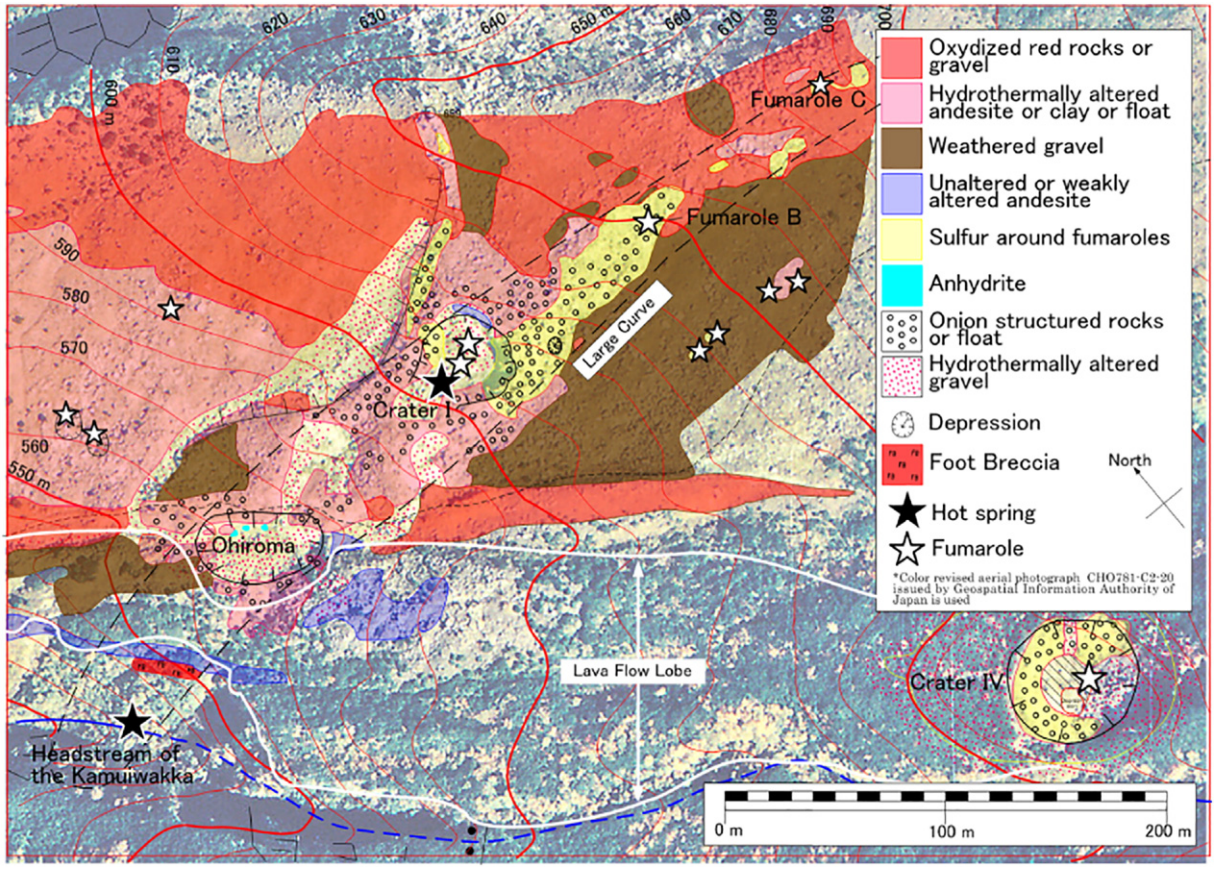

Fig. 3. Geological map around Crater I. Most of the area is covered by andesite floats of several meters' diameter and hydrothermally altered gravel. Aerial photographs CHO781-C2-20 from Geospatial Information Authority of Japan is used.

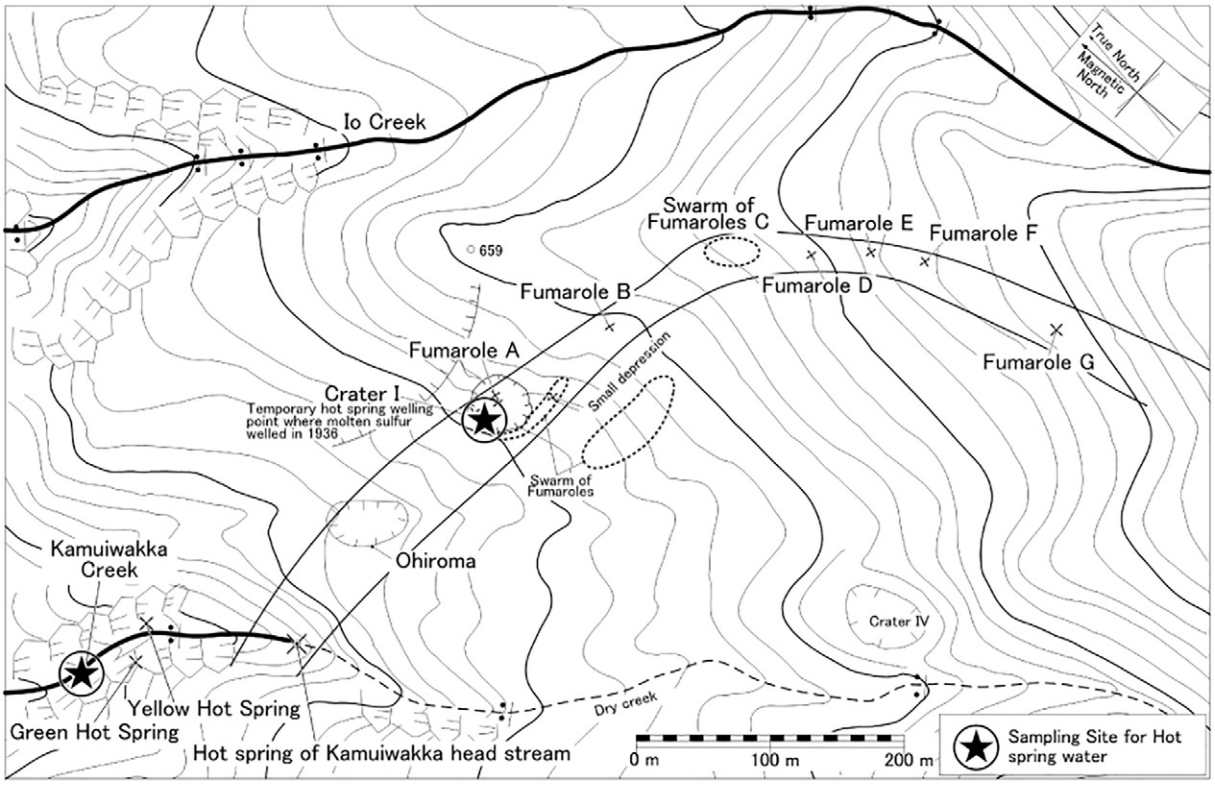

Fig. 4. Locations of collected hot spring water. The hot spring water at the Kamuiwakka Creek is a mixture of three hot spring waters: Yellow and Green and Kamuiwakka Head Stream hot springs.

Table 1
Analysis of hot spring water samples at Kamuiwakka Creek and Crater I. Cationswere analyzed by ICP - Atomic Emission Spectrometry. Anions were analyzed using ion chromatography.

Hot spring water analysis				
	Kamuiwakka Creek	Crater I		
	August 17, 2012	July 11, 2013		
Al	130	123.9	ppm	ICP
B	2.6	4.2	ppm	ICP
Ba	0.062	0.1	ppm	ICP
Ca	160	349.2	ppm	ICP
Fe	91	98.4	ppm	ICP
K	34.9	34.3	ppm	ICP
Mg	100	196.1	ppm	ICP
Mn	8.4	12.3	ppm	ICP
Na	150	229.6	ppm	ICP
P	1.3	1.4	ppm	ICP
Si	92	137.2	ppm	ICP
V	–	0.3	ppm	ICP
Y	–	0.2	ppm	ICP
Zn	–	1.3	ppm	ICP
Sr	0.62	–	ppm	ICP
F^-	18	35	mg/L	Ion chromatography
Cl^-	880	1500	mg/L	Ion chromatography
SO_4^{2-}	3000	4100	mg/L	Ion chromatography
pH=	1.5	1.3		
Temp.	44 °C	92 °C		

2.4. DC resistivity survey

A DC resistivity survey was conducted at 33 sites around Crater I, as depicted in Fig. 6. The electrical resistivity of the soil and rocks is determined mainly by groundwater that exists in the pores and cracks. For example, based on laboratory experiments, McCarter (1984) and Fukue et al. (1999) showed that the electrical resistivity of soils decreases when water contents increase. Therefore, the DC resistivity survey is effective to assess the surface underground structure and water veins. Results will suggest that hot spring aquifers exist underground near Crater I, where hot spring water was expelled in the summer of 2013 and 2014. Gas temperatures also have never exceeded the boiling point of water (100 °C), suggesting a sufficient amount of groundwater around Crater I. In addition to the conductive pore water, the clay minerals indicate low resistivity and have effects on the bulk resistivity of rock (e.g., Shevnin et al., 2007; Takakura, 2009).

In this study, a Wenner array was adopted for DC resistivity. Actually, 5 mm diameter brass rods with 25 cm length were used as electrodes. A 12 V-car battery with a DC-AC transformer was used as the current source. Two digital multimeters were used for voltage and current measurements.

The Fig. 6 shows that sites of DC resistivity survey were selected mainly at the bottom of Crater I and its eastern hill. At each site, a 30-m tape measure was stretched tightly straight along the slope and was fixed. Along the tape measure, at 15 m, the brass electrodes were inserted into the ground at various intervals: 0.2, 0.4, 0.6, 1, 1.4, 2, 3, 4, 6, 9, and 12 m. Resistivities were calculated using current and voltage values. Apparent resistivities were calculated as

$$\text{Apparent resistivity} = 2\pi aR,$$

where π signifies the circle ratio, a denotes the electrode interval, and R represents resistance (measured voltage amplitude divided by the injected current amplitude).

Data with voltage values of <0.01 mV were not used for additional analyses because the accuracies were suspect. The electrode intervals and apparent resistivities were used for analysis using inversion software IPI2Win provided by Moscow State University. Then the depth and resistivity of each layer were estimated.

3. Results

3.1. Observing aerial photographs and geological survey

For our study, we observed aerial photographs taken 2700 m above sea level in October 1978 after processing the photographs for color and sharpness.

Fig. 2 shows the adjusted aerial photographs. As might be readily apparent, in most cases, hot springs, craters, fumaroles, and oxidized spots are aligned considerably in a curve. We designate it as the "Large Curve" in this study. From west to east, the "Large Curve" starts at the head stream of Kamuiwakka Creek and passes through the Ohiroma Depression (Watanabe and Shimotomai, 1937). Then Crater I (collapse crater), Fumarole B (another small collapse in approximately 4 m diameter), Fumaroles C, D, E, F, and G. The extended area beyond Fumarole G is characterized as an area of less foliage, which strongly suggests that a special underground structure exists along this curve.

Some minor exceptional locations of fumaroles were recognized by field research in the southern part of the Fumarole B and 200 m west from Crater I. Those fumaroles were documented by Gochi (1985). Large white boulders of several meters in diameter are also concentrated along the "Large Curve." Those boulders have many deep cuts like those on limestone and holes in complicated decay.

Fig. 3 shows that the geology in this area is mostly composed of hydrothermally altered boulders, gravel, sand and clay. Those altered materials originally were apparently andesite lava sheets. Volcanic gas penetrated into cracks in the rock sheet and degraded it into onion-structured boulders, sand and clay. This process is ongoing; we recognized that two boulders had rolled down in 2013 at Crater I and 2015 at Fumarole B, respectively. The latter was of about 2 m diameter. A geological map issued by Hokkaido Disaster Prevention Conference showed the area around Crater I as covered by volcanic cinders (Katsui et al., 1982). However, no volcanic cinders were found from our geological survey.

Some part of the area of fumaroles along the "Large Curve" to the east of Crater I was covered by sulfur cement: a mixture of sulfur and hydrothermally altered sand or clay on gray, partially hardened ground. The area near Crater I is mostly covered by white boulders.

A lobe of andesite lava is recognized along the northern bank of Kamuiwakka Creek (Fig. 2). Andesite rocks in the lobe are less altered than the rocks around Crater I. It is readily apparent that the lava lobe had flowed after the surrounding andesite sheet. Downstream of the andesite lobe is lost at Kamuiwakka Creek. In addition, at Ohiroma, a part of the lobe is lost by collapse. This is evidence from which we infer that the Ohiroma depression can be regarded as a collapse crater.

3.2. Hot springs analysis

Hot spring water in Kamuiwakka Creek and Crater I was collected at the point portrayed in Fig. 4. As presented in Table 1, the compositions of both hot waters at Kamuiwakka and Crater I show good agreement. The water sample in Kamuiwakka Creek contains three hot spring waters flowing from upstream (Fig. 4; "Yellow Hot Spring" = 79 °C, pH = 1 on July 7, 2013; "Green Hot Spring" = 41 °C, pH = 2 on July 7, 2013; the Headstream of the Kamuiwakka = 27.6 °C, pH = 3 on July 5, 2013). The hot spring at Crater I (92 °C, pH = 1.3, July 11, 2013) was expelled, forming a small stream on the crater bottom of approximately 20 m length on the surface temporarily during the summers of 2013 and 2014. The streambed in the first 2 m from the welling point was covered by spicula sulfur crystals. Farther downstream, it was free from sulfur crystals.

Both samples have low pH and strong acidity. Roughly speaking, their compositions are analogous, which suggests that those hot spring waters derive from a common source (Table 1). We also found some

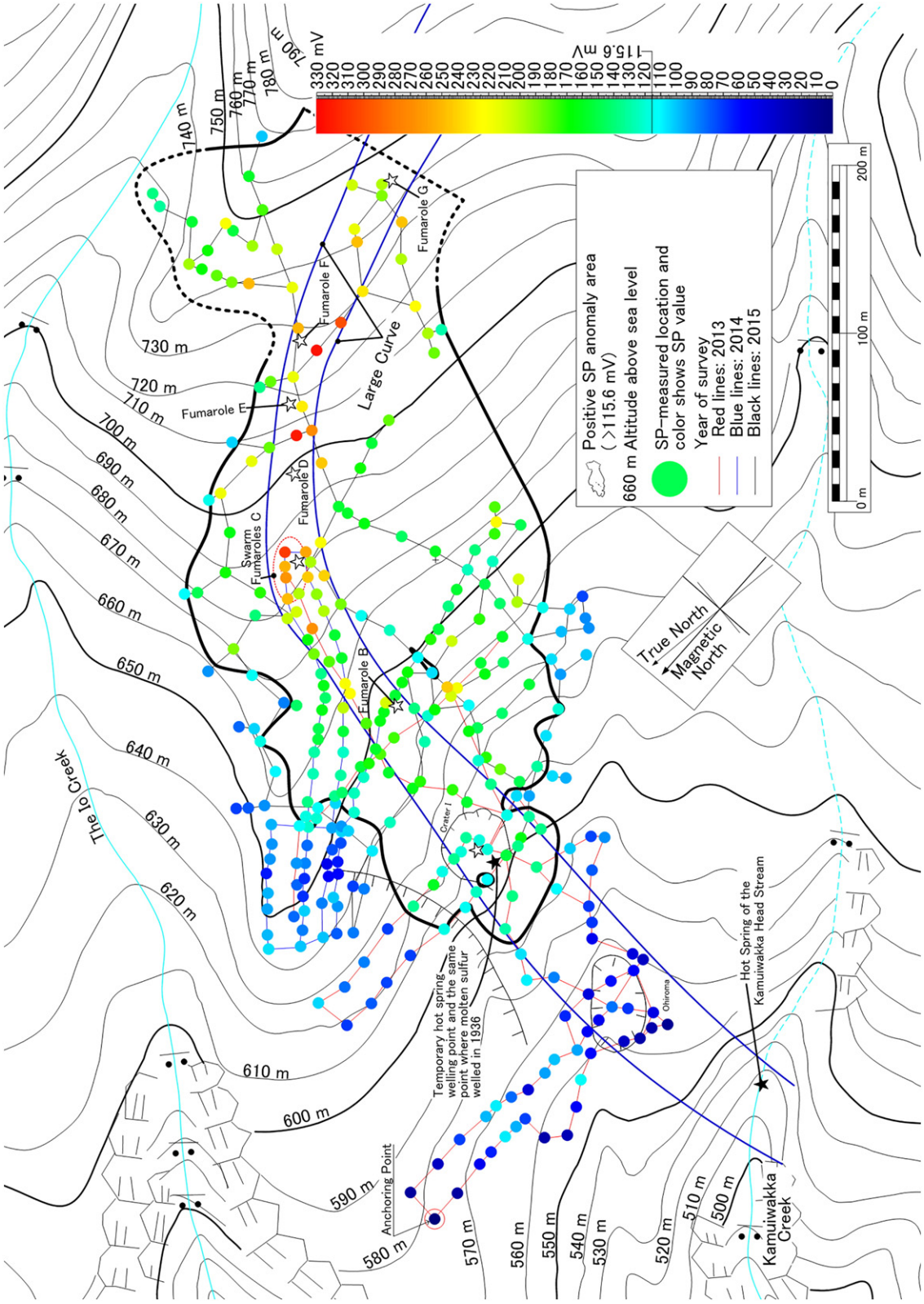

Fig. 5. Map of Self-potentials (SP). Altitude effects of SP were offset here. An area with SP higher than 115.6 mV is shown in the enclosure of the curve.

discrepancies. The sample at Kamuiwakka Creek contains a small amount of Sr, whereas the hot spring at Crater I exclusively contains V, Y, and Zn, although those amounts are as low as 0.2–1.3 ppm.

It is noteworthy that the ratios of SO_4^{2-} and Cl^- are strikingly high in three or four orders of magnitude in both samples. The pH is extremely low.

As described above, the hot spring waters were expelled temporarily at the center of Crater I in the summers of 2013 and 2014. While the hot spring waters were expelled, the gas emissions at a fumarole located approximately 10 m east of and 6.2 m higher than the hot spring welling point were suspended. When the hot spring waters ceased, the fumarole restarted gas emissions. This central fumarole is one of the two

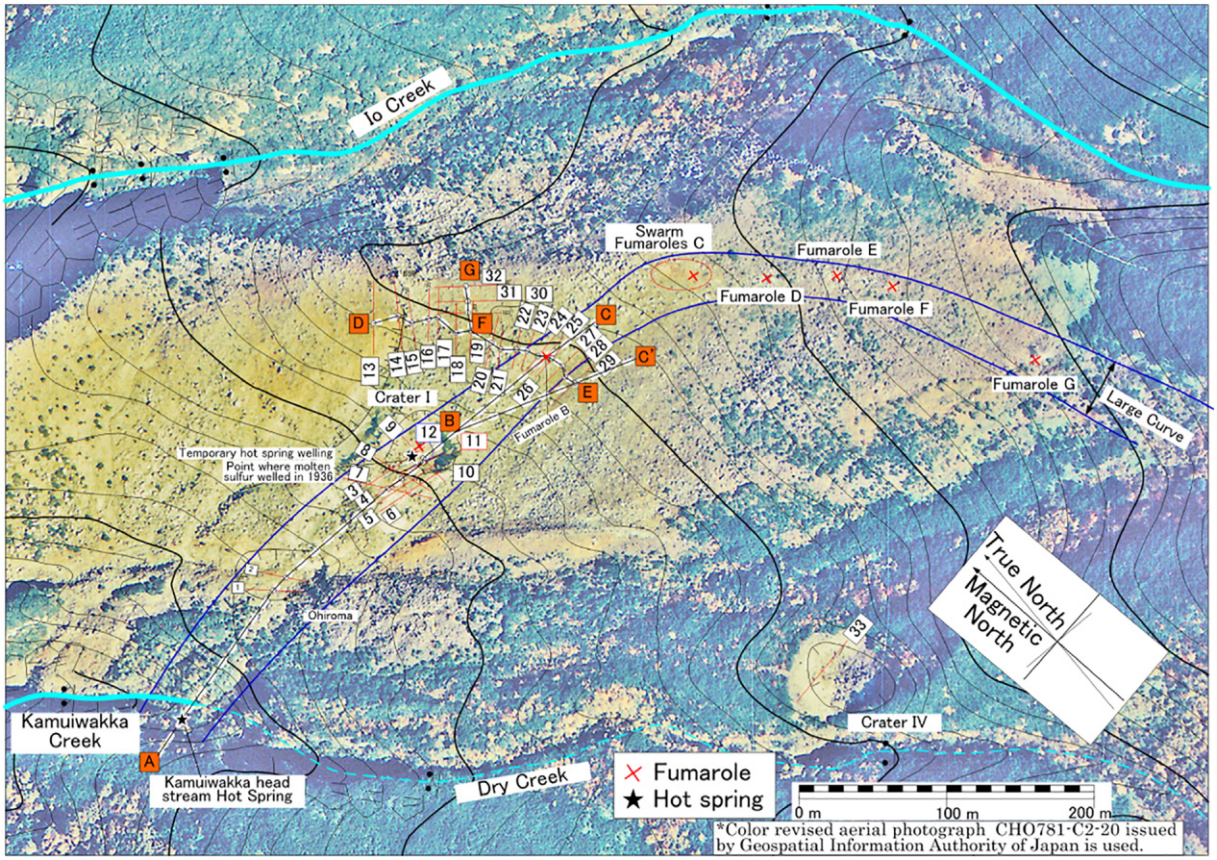

Fig. 6. Site locations of DC resistivity surveys. Electrodes for survey are arranged along each thin red line at each site. Thick white broken lines with narrow solid black lines show locations of resistivity sections. Aerial photographs CHO781-C2-20 from Geospatial Information Authority of Japan is used.

most active fumaroles in Crater I with the other fumarole located approximately 8 m east and 3.5 m higher than the central fumarole. Although the central fumarole halted its activity, the other larger fumarole remained active as usual. Several other smaller fumaroles exist in the crater. Their activities are weak but still active while the hot spring waters are expelled.

3.3. Self-potential survey

A self-potential survey (SP survey) was conducted during the summers of 2013, 2014, and 2015. The observed SP data clearly indicate the altitude effect. The SP values and the altitude of measuring points indicate a mutually negative correlation, mainly because of the groundwater flow along the mountain slope of the survey area (Goto et al., 2012). It is noteworthy that a negative correlation between raw SP values and altitude is very obvious from 600 to 655 m above sea level, while a clear positive correlation is found at the elevation lower than 600 m or higher than 655 m. To remove the altitude effect on SP and extract the SP distribution closely related to the hydrothermal activities, we focused the SP values at the elevation between 600 and 655 m, and estimated an equation of correlation incorporating altitude and SP in this region using least-squares method.

$$Y = -0.6928H + 383.61$$

In that equation, Y is the altitude-related-SP value; H is altitude at the point of SP measurement, and R^2 is 0.88. With this function, we removed the altitude-related-SP from the all observed raw SP, and calculated the altitude-corrected values (Fig. 5). The anchoring point (reference of SP measurement), where the SP value is zero, is located at the northwestern end of the SP survey area, as marked in Fig. 5. As a result, high SP values are found at the eastern uphill of Crater I. Here we define a "positive SP anomaly area" using the threshold value of 115.6 mV because the lowest value of SP at fumarole swarm was 115.6 mV in Crater I. The positive SP anomaly area is presented in Fig. 5.

The positive SP anomaly area corresponds well to the "Large Curve" with its many fumaroles. Especially, the SP values are quite high within the "Large Curve." Values higher than 300 mV are found near the Fumarole F, between the Fumaroles D and E, and in the swarm Fumarole C. These extremely high-SP areas are located 200 m–300 m to the east of Crater I, at some distance from the molten sulfur eruption site. Values at other points around those locations are also extremely high; most of them are higher than 200 mV.

However, the SP values in and around Crater I are lower. Most locations in Crater I show a slightly higher value than 156 mV. At the middle of Crater I, the value is <115.6 mV (110.5 mV). Although Crater I has two large fumaroles and several other small fumaroles emitting volcanic gas, the SP values are not high relative to those of the other fumaroles.

It is noteworthy that there are some hot spots at which values were higher than the surrounding locations, e.g. southeast of fumaroles B and D, outside of the "Large Curve." At some cold spots, the values are lower than those of surrounding locations.

3.4. DC resistivity survey

We conducted a DC resistivity survey (Wenner-array method) at 33 sites (Fig. 6). The major obtained resistivity models are presented in Fig. 7, together with an example of the apparent resistivity curve. Unfortunately the observed error at site 14 was quite large and excluded from Fig. 7. Sites 3, 5, 8 10, 11, and 12 indicated similar results to those shown in Fig. 7 but were omitted, as the figure shows, because these sites are not located along the profiles.

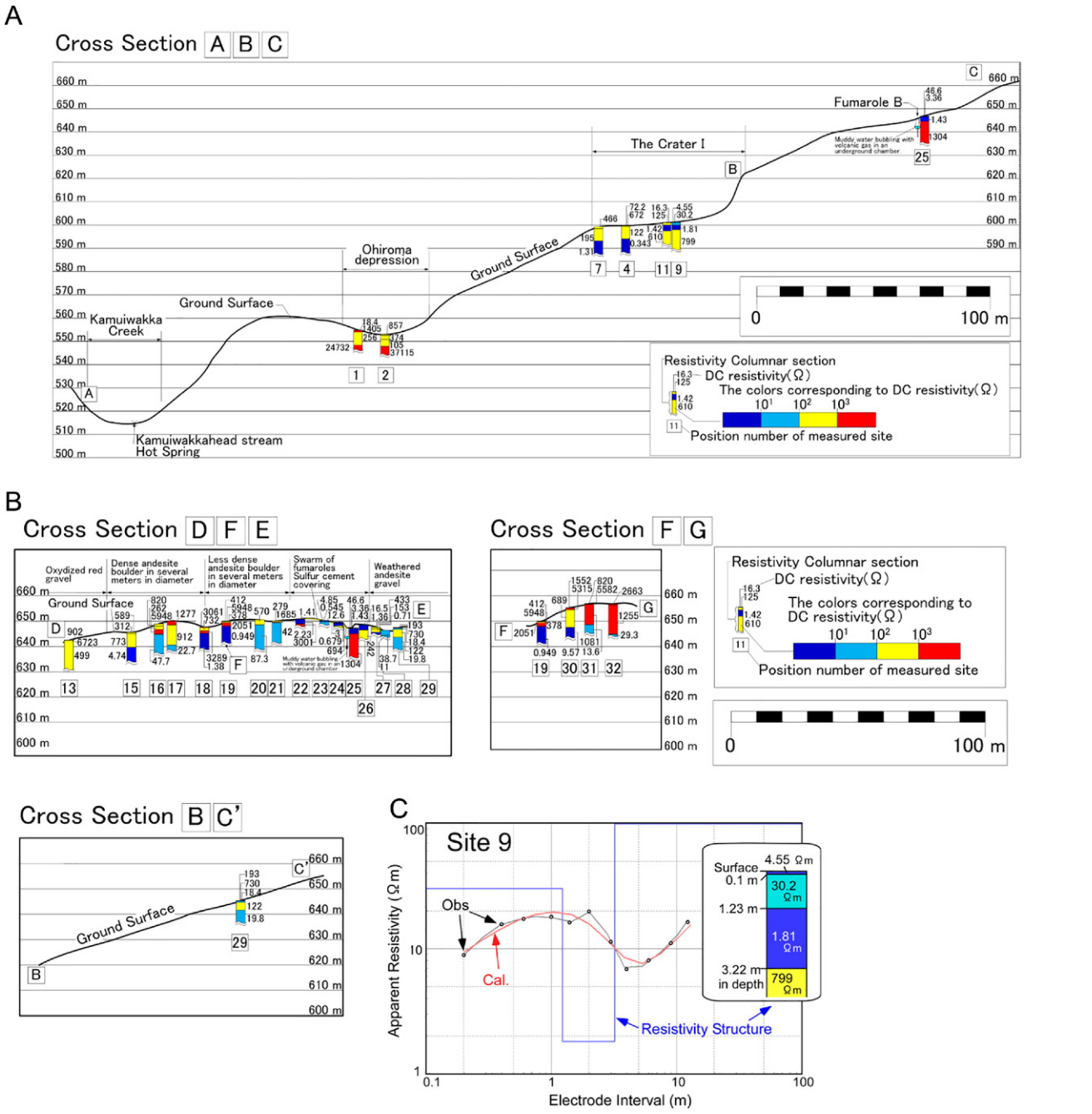

Fig. 7. Results of the DC resistivity survey. Locations in Crater I (sites 4,7,9 and 11) show extremely low resistivity as dark blue below the crater bottom, which implies the presence of hot spring water (figure a). Several other locations also show low resistivity (figures in b). Panel c presents examples of apparent resistivity curves (black = observed, red = calculated by IPI2WIN).

Sites 4 and 7, 9, and 11 show extremely low resistivity similar to the resistivity of seawater. Those data suggest the existence of hot spring water 5–6 m below Crater I's bottom at sites 4 and 7, and 1 or 2 m, respectively, below sites 9 and 11. Sites 27–29 in section D–E show moderately low resistivity at 3–5 m below the ground surface. Those data imply the possibility of existence of groundwater. Sites 15–21 also show low resistivity. It seems that they might be attributable to hot spring aquifers. At sites 22–26, mostly in the "Large Curve," the ground surface comprises hydrothermally altered clay, which is covered by sulfur cement. Clay minerals indicate high electrical conduction, and are apparently a cause of extremely low resistivity near the surface at these sites.

Sites 22 and 25 also show high resistivity layers below the low resistive surface. Because the sites are in a fumarole swarm, the high value should be related to gas and unsaturated cavities under the ground. In fact, at site 25 on Fumarole B, we found a near-surface large cavity that was apparently several meters deep under the bottom of the collapsed ground. It is based on our field observation, with the sound of mud bubbling below the surface (bubbling was observed visually in May 2010). Furthermore, around Fumarole B, "drum-like" sounds were observed. These suggest that a cause of high resistivity is due to many small unsaturated cavities near the surface, though there is a possibility of dry hot ground as another cause. Sites 19, 30, 31, and 32 in sections F–G also show extremely low resistivity 8–11 m below the surface. Aquifers might exist at these sites too, similar to the other sites. Resistivity of soil saturated with brine corresponds to these values.

High resistivity values were found around 5–6 m below the bottom of Ohiroma depression at sites 1 and 2. The Ohiroma depression is

surrounded by hydrothermally altered andesite, clay and float as shown in the geological map (Fig. 3), which show low resistivity. The high resistivity might indicate less altered andesite volcanic rock sheet and/or anhydrite based on the geological observations, or cavities below the depression similar to at Sites 22 and 25.

4. Discussion

Based on our observed results and interpretations, we investigated possible mechanisms of molten sulfur eruption at Mt. Shiretokoiozan. Some volcanoes gush molten sulfur, but no other volcano produces such large sulfur eruptions as those at Mt. Shiretokoiozan.

In our SP result (Fig. 5), the high positive SP anomaly area is located not in Crater I; the peak of the positive SP anomaly has an offset from Crater I (about 200 m to the east). The SP distribution does not support active venting beneath Crater I. The hypothetical model of sulfur eruption as presented by Watanabe (1940) needs two factors; a sulfur-containing chamber under the Crater I, and sulfur deposits forming the walls of chamber. The later can be made from upwelling hot water/steam beneath the Crater I. The vapor pressure also propels the molten sulfur eruption (Watanabe, 1940). Although there is a possibility of huge chamber beneath the Crater I, the upwelling water/gas cannot be expected here, and the hypothesis should be reconsidered.

We propose that sulfur has been produced not from the large chamber beneath Crater I, but from other places. Based on our multidisciplinary results, the eastern area of Crater I (Fig. 5) is a candidate location. This area is characterized by its positive SP anomaly, correlating with upwelling groundwater zones and underlying heat sources. If volcanic gas is supplied to the aquifer below this area, several chemical components can dissolve in the groundwater and generate elementary sulfur. Analogous phenomena in the lake Poas in Costa Rica and Yugama in Japan have been described by Francis et al. (1980) and Takano et al. (1994) respectively. That inference is supported by results of our chemical analyses of hot spring water expelled at Crater I and the Kamuiwakka creek with concentration of ions H^+, Cl^-, F^- and SO_4^{2-}. In this case, the sulfur deposits might be stored in the aquifer or in small voids. Here, we suggest a hypothetical scenario of possible molten sulfur eruption at Mt. Shiretokoiozan: i) the sulfur deposits are stored in the eastern area of Crater I; then ii) when the volcanic activity of Mt. Shiretokoiozan becomes more active, the stored sulfur melts and flows below the surface and reaches Crater I as molten sulfur.

To assess the probability of our hypothetical scenario for sulfur eruption, we specifically examine two questions in the following sections: i) Where is the sulfur precipitated and stored in this hypothesis? ii) Can the predicted amount of sulfur in this hypothesis explain the amount of erupted sulfur observed in 1936?

4.1. Sulfur generation in the aquifer

We suggest a shallow aquifer widely existing below Crater I and the surrounding area (along the "Large Curve"). For example, hot spring waters were temporarily expelled in the summers of 2013 and 2014 in Crater I. Our DC resistivity survey indicates a low resistivity layer under the bottom of the crater (Fig. 7), which suggests the existence of an aquifer. Similar low resistive layers were found at other sites by our DC resistivity surveys, implying a wide aquifer at the shallow depth. The results of SP survey support the wide aquifer. The positive SP anomaly area to the east of Crater I (Fig. 5) implies a large amount of upwelling groundwater, but no spring except for Crater I was observed. The observed raw SP value includes the altitude effect (Section 3.3) caused by groundwater flow along the mountain slope. Therefore, the upwelling groundwater in the eastern area of Crater I seems to flow down along an aquifer distributed widely below the slope, as shown in Fig. 8. Chemical components and gas temperature data also support the existence of a wide aquifer. In the positive SP anomaly area, especially along the "Large Curve," gas emission is active. As this report described, SO_4^{2-}, Cl^-, F^- and H^+ were contained in the hot spring water. The fumarole temperature never exceeded 100 °C, or the boiling point of the water. These results imply that the gases are passing through a widely distributed aquifer and that some gas components dissolve into the groundwater.

Our analyses of hot spring water yielded results that were consistent with the existence of a wide aquifer. Along Kamuiwakka Creek (Fig. 4), we identified three hot springs located west of Crater I: Hot Spring of the Kamuiwakka Headstream, "Yellow Hot Spring" and "Green Hot Spring" (Fig. 4). They apparently originated from the altered andesitic block. The total amount of water flow from these hot springs was measured for this study at the downstream side, where Kamuiwakka Creek water was collected as portrayed in Fig. 4. The approximate flow rate was about

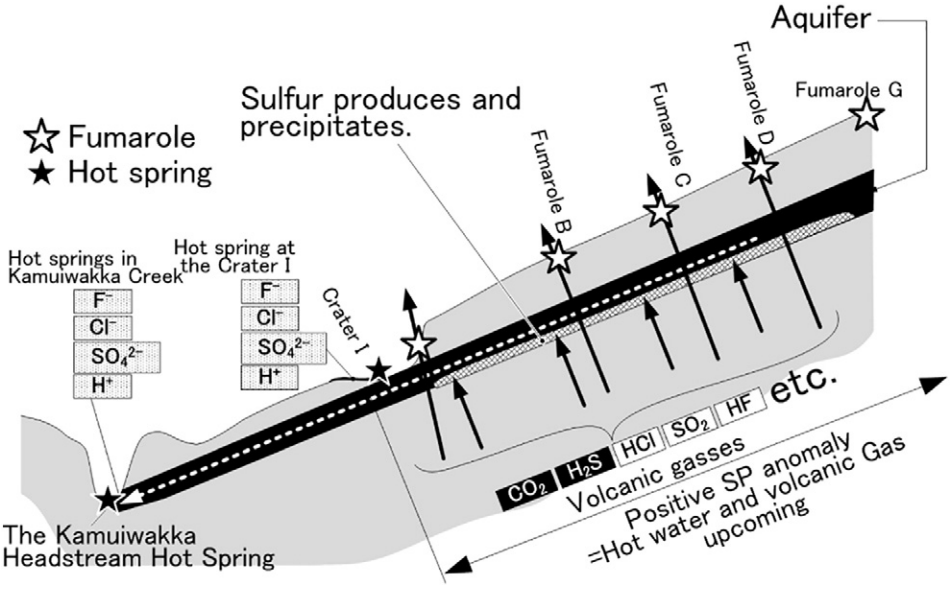

Fig. 8. Schematic view of hypothetical model of sulfur concentration in the survey area. Our model has an aquifer in this area, with volcanic gases (solid thick arrows), consisting of water soluble (white rectangles) and weakly soluble ones (black rectangles). Some gases dissolve into the underground water. The reaction between hydrogen sulfide and sulfur dioxide generates and precipitates sulfur in the aquifer over many years.

1164 t/day or 424,940 t/yr. Results of geochemical analyses indicate the similarity of water at Crater I and Kamuiwakka Creek (Table 1). The Upper Kamuiwakka Creek from the headstream is dry, with no water flow or springs. The SP map (Fig. 5) also indicates a lack of large positive SP anomalies at areas down-slope from Crater I. Therefore, although the source of Kamuiwakka hot springs is unknown, it might come from a widely distributed aquifer between Crater I and Kamuiwakka Creek (Fig. 8).

Based on our DC resistivity survey, we estimated the porosity of the aquifer below Crater I. The average bulk resistivity of the aquifer (sites 4, 7, 9, and 11 in Fig. 7) was 1.2 Ωm. The resistivity of the hot spring water from Crater I, measured in our laboratory, was 0.29 Ωm at 20 °C. Because the hot spring water's temperature was 92 °C, the water resistivity at sampling (ρ_{92}) was inferred from the following equation by Dakhnov (1962) as

$$\rho_{92} = \rho_{20}/(1 + 0.02(T_{92} - T_{20})).$$

Because $\rho_{20} = 0.29$ (Ωm), $T_{92} = 92$ (°C), $T_{20} = 20$ (°C) in this study, the calculated resistivity of hot water at 92 °C is about 0.12 Ωm. For porosity estimation, we used Archie's law (Archie, 1942); $\rho = \rho_w \Phi^{-m}$, where Φ denotes the porosity, m signifies cementation factor (normally 2 for porous media), ρ_w denotes resistivity of the pore water (0.12 Ωm), and ρ stands for the bulk resistivity of rock (1.2 Ωm). In this case, the aquifer porosity is estimated as approximately 30%. The cementation factor has ambiguities, and m can be 1.5–2.5. In this case, the range of estimated porosity is about 20–40%. Consequently, large pore spaces seemed to distribute in the aquifer below Crater I. Similar formation resistivity (0.7–20 Ωm) was found at another site of our DC resistivity survey, corresponding to porosity of about 3–50% (in the case of $m = 1.5$–2.5). For these porosity estimations, clay contents should be taken into account, however, there is no information of clay content in this region. Although the borehole-based lithological studies are necessary for more quantitative estimation of porosity, we roughly consider that the widely distributed aquifer in this survey area, suggested above, has porosity of about 3–50% (typically 30%). Lower porosity (e.g., 3%) can be a representative value in the case of high clay content.

A widely distributed shallow aquifer with high porosity can be a reservoir of sulfur deposits. If the volcanic gas including sulfur content has been supplied to an aquifer (as in our hypothetical model, Fig. 8), the following chemical reaction of hydrogen sulfide and sulfur dioxide produces sulfur in water as (Yamamoto, 1973)

$$2H_2S + SO_2 \rightarrow 2H_2O + 3S.$$

Sulfur is also produced in other ways, as (Yamamoto, 1973)

$$2FeCl_3 + H_2S \rightarrow 2FeCl_2 + 2HCl + S.$$

Watanabe and Shimotomai (1937) also described sulfur as generated by the reaction between hydrogen sulfide and sulfur dioxide in the aquifer. As this report described high density of Cl^-, SO_4^{2-} and some F^- were found in the low pH hot spring water in Kamuiwakka Creek, which implied that the volcanic gases dissolve into ground water.

4.2. Estimation of the volume of sulfur reserved in aquifer

Based on the hypothesis of sulfur precipitations (Fig. 8), we can roughly estimate the total amount of sulfur in the aquifer. Here, we assume that sulfur has been generated and precipitated in the shallow and wide aquifer under the positive SP anomaly area (>115.6 mV), as presented in Fig. 5, with area of 79,950 m^2. Note that the estimation depends essentially on the SP data in the western side of survey area, so that it is a kind of the minimum value. Unfortunately, no information related to the aquifer thickness was obtained from our DC resistivity surveys and no borehole data is available. From our geological survey, a hot spring welling layer on the eastern bank of Kamuiwakka Creek has approximately 4 m thickness. Therefore, we simply assume the aquifer thickness as 4 m as the least value. Consequently, the total volume of the aquifer would be 319,800 m^3 or more. The sulfur can be reserved in the pore spaces in the aquifer. If the average porosity of the aquifer is 3–50% (typically 30%) as discussed, and if all pore spaces would be filled by precipitated sulfur, then the potential volume of sulfur in the aquifer is calculable as about 9600–160,000 m^3 or 19,000–320,000 tons (typically 96,000 m^3 or 190,000 tons). The observed amount of sulfur that gushed out in 1936 was approximately 116,523 tons, as described, with volume of 58,262 m^3. Consequently, the inferred total amount of the sulfur in the aquifer is 0.2–2.7 (typically about 1.6) times as large as the erupted amount in 1936. Note that this is the minimum inferred value since the area and thickness of aquifer are based on the limited known data.

It is noteworthy that Crater I is located at the lowest altitude part of the positive SP anomaly area (Fig. 5). Therefore, in our hypothetical model (Fig. 8), we presume that higher volcanic activities activate the melting of the precipitated sulfur in aquifer below the positive SP anomaly area, activate the flowing down of molten sulfur, and activate the eruption at Crater I. The important factor validating our model (Fig. 8) is the flow velocity of the molten sulfur in the aquifer. If the subsurface flow velocity of the molten sulfur had not been sufficient, the amount of the erupted sulfur in our model would have been less than the amount that was documented at the sulfur eruption in 1936. Our hypothesis would therefore be rejected.

First, we adopted Darcy's law to derive the velocity of a liquid flowing in the aquifer (cm/s) as $v = k \times i$, where k denotes the hydraulic conductivity of the aquifer (cm/s) and where i is the hydraulic gradient. In this study, k is assumed simply as 0.14 because the survey area is mostly covered by gravel (Fig. 3) and because the aquifer porosity is inferred as 30% typically. Hydraulic conductivity of the gravel filled by water is typically 1.0 and larger (e.g., Bear, 1972). The viscosity of liquid sulfur at 157 °C is about 7 times greater than that of water at 20 °C (Steudel, 2003); $k = 1.0/7 = 0.14$. Hydraulic gradient i is derived as 0.38 based on the averaged slope angle in the eastern area of Crater I (about 21°). Then the flow velocity of molten sulfur, v, can be estimated as about 0.5 mm/s, which means that the daily flow distance is about 40 m.

The daily erupting volume of molten sulfur at Crater I can be estimated based on our hypothetical model in Fig. 8. The Crater I diameter is approximately 40 m, but its bottom width is about 10 m. We presume that the exit of the aquifer to the Crater I has 10 m width and 4 m thickness. Then, based on the daily flow distance of sulfur (40 m), porosity of the aquifer (30%), and the aquifer exit size (4 × 10 m), the daily erupted volume is $40 \times 0.3 \times 4 \times 10 =$ about 500 m^3. The total volume of the four-day eruption is also estimated as about 2000 m^3, as shown in Fig. 9. This final estimation is comparable to the tangible amount of approximately 1759 m^3, which welled in every four days in 1936 (Watanabe, 1940).

Although these estimations include ambiguities such as the thickness, porosity, and hydraulic conductivity of the aquifer, we conclude that our hypothetical model cannot be rejected. Our model presented in Fig. 8 can explain most of the observed features of geological settings, geophysical and geochemical surveys, total amount of erupted molten sulfur, and also the amount of occasional eruption every four days. It is noteworthy that our model does not contradict the existence of small sulfur chambers beneath Crater I, as proposed by Watanabe (1940). Moreover, our model is rather amenable to such buried chambers. As described, volcanic activity and heating can initiate the melting of sulfur deposits in the aquifer below the positive SP anomaly area. If the molten sulfur flowing down in the aquifer can be stored in a small chamber below the Crater I (about 2000 m^3, for example), the observed geyser-like eruption of molten sulfur (Watanabe, 1940) can be explained. Not only the increased volcanic activities but other causes responsible for eruptions are also inferred since the surface temperature of steam vents in the area is close to 100 °C, and sulfur may have kept the liquid condition in the aquifer. Shaking by a seismic event or over-pressuring

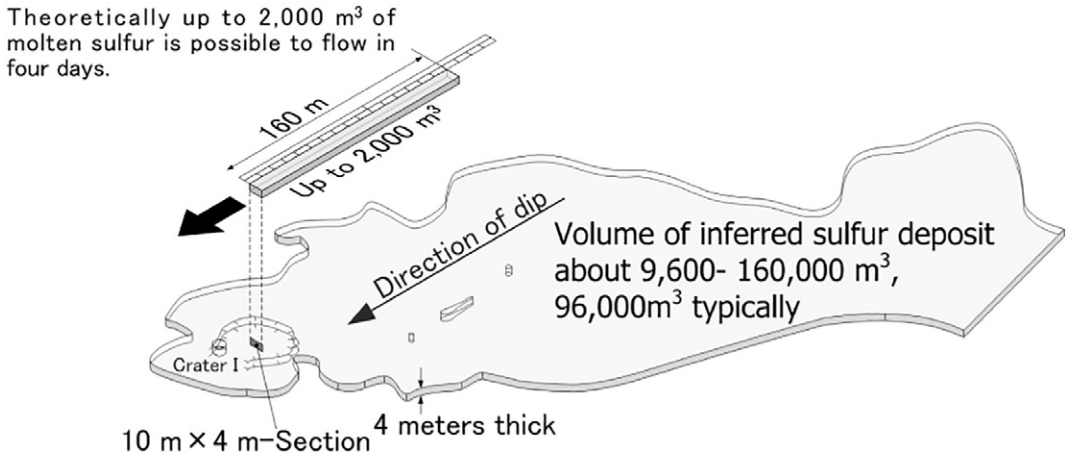

Fig. 9. Schematic drawing of aquifer below the positive SP anomaly area. The inferred volume of sulfur deposits in this area is shown with the inferred volume flowing into Crater I in four days.

of local steam is also a candidate of initiation of molten sulfur eruptions. Further observations such as geophysical mapping to create images of the distribution of aquifers below the survey area, together with sampling from shallow boreholes, are expected to indicate which mechanism is dominant for explaining the molten sulfur eruptions.

5. Summary

Together, these multidisciplinary surveys, aerial photographs, geological surveys, geochemical analyses of hot springs, self-potential or streaming-potential (SP) surveys, and DC resistivity survey have elucidated near-surface groundwater information. Based on our observation results and interpretations, we can propose a possible mechanism of molten sulfur eruption at Mt. Shiretokoiozan. We infer that a shallow aquifer exists widely below Crater I and the surrounding area, especially along the "Large Curve." We propose that the sulfur is generated and precipitated in the aquifer by a reaction between upwelling gases and hot water. When the volcano is active, the sulfur in the aquifer is pushed by expansion of water vapor and expelled.

To establish our hypothesis, using our results of SP and DC resistivity values and hot water conductivity, we calculated the porosity of the aquifer below Crater I. We estimated the potential amount of sulfur stored in the aquifer as about 9600–160,000 m^3 or 19,000–320,000 tons (typically 96,000 m^3 or 190,000 tons) at least, based on the several assumptions. Our estimation is well comparable to a part or the whole part of the tangible amount of expelled sulfur 58,262 m^3 or 116,523 tons from the 1936 eruption. We also estimated the amount of sulfur expelled during four days as approximately 2000 m^3, which is closely comparable to the tangible amount of 1759 m^3 of four days during the 1936 eruption.

This evidence demonstrates that our estimation and hypothesis do not contradict the observed phenomena related to the 1936 eruption.

Acknowledgement

The authors greatly appreciate the Prof. Alessandro Aiuppa, and two anonymous reviewers for their comment. This work is partly supported by JSPS Grants-in-Aid for Scientific Research(B), No.26289347, and a grant from the Ministry of Education, Culture, Sports, Science and Technology (MEXT), Japan for the "Development of new tools for the exploration of seafloor resources" project.

References

Archie, G.E., 1942. The electrical resistivity log as an aid in determining some reservoir characteristics. Trans. Am. Inst. Min. Metall. Pet. Eng. 146, 54–62.
Barde-Cabusson, S., Finizola, A., Peltier, A., Chaput, M., Taquet, N., Dumont, S., Duputel, Z., Guy, A., Mathieu, L., Saumet, S., Sorbadere, F., Vieille, M., 2012. Structural control of collapse events inferred by self-potential mapping on the Piton de la Fournaise volcano (La Reunion Island). J. Volcanol. Geotherm. Res. 209, 9–18.
Bear, J., 1972. Dynamics of Fluid in Porous Media. Elsevier, New York (764 pp.).
Corwin, R.F., Hoover, D.B., 1979. The self-potential method in geothermal exploration. Geophysics 44 (2), 226–245.
Dakhnov, V.N., 1962. Geophysical well logging. Q. J. Colorado Sch. Min. 57-2 (445 pp.).
Francis, P.W., Thorpe, R.S., Brown, G.C., Glasscock, J., 1980. Pyroclastic sulphur eruption at Poás volcano, Costa Rica. Nature 283 (5749), 754–756.
Fukue, M., Minato, T., Horibe, H., Taya, N., 1999. The micro-structures of clay given by resistivity measurements. Eng. Geol. 54 (1), 43–53.
Geological Survey of Japan, 1967. Metallic and Non-metallic Mineral Deposits of Hokkaido (in Japanese).
Gochi, N., 1985. Outlines of Lectures at Hokkaido Branch of Geology Society of Japan.
Goto, T., et al., 2012. Implications of self-potential distribution for groundwater flow system in a nonvolcanic mountain slope. Int. J. Geophys. 2012, 10.
Harris, A.J., Sherman, S.B., Wright, R., 2000. Discovery of self-combusting volcanic sulfur flows. Geology 28 (5), 415–418.
Ishido, T., 1989. Self-potential generation by subsurface water flow through electrokinetic coupling. Detection of Subsurface Flow Phenomena. Lecture Notes in Earth Sciences vol. 27, pp. 121–131.
Kadokura, S., 1919. Geological Survey in Shiretoko Peninsular, Report of Mineral Explorations 47 pp. (in Japanese; the Japanese title, "Shiretokohanto Chishitsuchosa Houbun. Kobutsu Chosa Houkoku" (in Japanese) is Translated by the author, M. Y.).
Katsui, Y., Yokoyama, I., Okada, H., Takagi, H., 1982. Shiretoko-iozan, Its Volcanic Geology, History of Eruption, Present State of Activity and Prevention of Disasters, Research Reports of Volcanoes in Hokkaido. vol. 8. Committee for Prevention of Disasters in Hokkaido (in Japanese) (98 pp.).
McCarter, W.J., 1984. The electrical resistivity characteristics of compacted clays. Geotechnique 34 (2), 263–267.
Shevnin, V., Mousatov, A., Ryjovand, A., Delgado-Rodriquez, O., 2007. Estimation of clay content in soil based on resistivity modellingand laboratory measurements. Geophys. Prospect. 55, 265–275.
Skinner, B.J., 1970. Sulfur lava flow on Mauna Loa. Pac. Sci. 24 (1), 144–145.
Steudel, R. (Ed.), 2003. Elemental Sulfur and Sulfur-rich Compounds I. Springer, New York (206 pp.).
Takakura, S., 2009. Influence of Pore-water Salinity and Temperature on Resistivity of Clay-bearing Rocks, BUTSURI-TANSA, (Exploration Geophysics) 62, 4, 385–396 (in Japanese with English abstract).
Takano, B., Saitoh, H., Takano, E., 1994. Geochemical implications of subaqueous molten sulfur at Yugama crater lake, Kusatsu-Shirane volcano, Japan. Geochem. J. 28 (3), 199–216.
Theilig, E., 1982. A Primer on sulfur for the planetary geologist. NASA Contract. Rep. 3594, 19–28.
Watanabe, T., 1940. Eruption of molten sulphur from Siretoko-iosan Volcano, Hokkaido, Japan. Jpn. J. Geol. Geogr. 17, 289–310.
Watanabe, T., Shimotomai, T., 1937. Volcanic activity of Shiretokoiozan, Kitaminokuni. 1936, Bulletin of Hokkaido Geological Survey. vol. 9 37 pp. (in Japanese ; the Japanese title "Kitaminokuni Shiretokoiozan showajuichinenno katsudou. Hokkaido Chishitsu Chosakai Hokoku 9" is translated by the author, M. Y.).
Yamamoto, D., 1973. Encyclopedia of Chemical Experiment, P244, P250.
Yamamoto, M., 2017. Explosive eruption which blew out molten sulfur at the Crater I on Volcano Shiretokoiozan. Bulletin of the Shiretoko Museum. vol. 39, pp. 1–20.
Yamamoto, M., Goto, T., 2015. Near surface structure of a Crater on mountain side of Mt. Shiretokoiozan and its mechanism of molten sulfur eruption. Proceedings for the Poster Session at Japan Geoscience Union in 2015.
Zlotnicki, J., Nishida, Y., 2003. Review on morphological insights of self-potential anomalies on volcanoes. Surv. Geophys. 24, 291–338.